35th Annual International Conference of the IEEE EMBS
Osaka, Japan, 3 - 7 July, 2013

Automated Signal Pattern Detection in ECG During Human Ventricular Arrhythmias

K. Balasundaram[1], S. Masse[2], K. Nair[2], K. Umapathy[1]

Abstract— **Ventricular arrhythmias seriously affects cardiac function. Of these arrhythmias, Ventricular fibrillation is considered as a lethal cardiac condition. Recent studies have reported that ventricular arrhythmias are not completely random and may exhibit regional spatio-temporal organizations. These organizations could be indicative of reoccurring signal patterns and might be embedded within the surface electrocardiograms (ECGs) during ventricular arrhythmias. In this work, we aim to identify such reoccurring ECG signal patterns during ventricular arrhythmias. The detection of such signal patterns and their distribution could be of help in sub-classifying the affected population for better targeted diagnosis and treatment. Our analysis on 14 ECG segments (on average 3.24 minutes per segment) obtained from the MIT-BIH ventricular arrhythmia database identified three reoccurring signal patterns. A wavelet based technique was developed for automating the pattern identification process using ECGs. The proposed method achieved automated detection accuracies of 73.3%, 75.0% and 86.6% for the proposed signal patterns.**

Index Terms— **Ventricular Arrhythmia, Pattern Detection, Wavelet Transform, Signal Processing**

I. Introduction

Sudden cardiac death remains as one of the leading causes of death, with rates as high as 400,000 in the U.S. annually [1]. Ventricular fibrillation (VF) is one of the causes of sudden cardiac deaths that has demanded a great deal of attention. This is primarily because there is still very little information with regards to the mechanisms that distorts the coordinated ventricular activity of the heart. The study of ventricular arrhythmias has been focused to VF due to its lethal nature. Historically, VF has been considered to be a combination of multiple chaotic wave fronts of electrical excitation [2], but recent studies have disputed this notion that VF is completely random.

The study into rotor dynamics has shown that there is some form of organization that can provide mechanistic insights for the arrhythmia [3]. Relating these organizational centers to surface electrocardiogram (ECGs), surface ECGs during ventricular arrhythmias might be embedded with the influence of these migrating organizational centers in the form of reoccurring signal patterns with varying degree of temporal organization. An analysis of the ECG signal patterns during ventricular arrhythmia could reveal different distribution of reoccurring signal patterns that may be associated to different sub-groups of affected population. Our previous works [4], [5] performed classification of ventricular arrhythmias using wavelet based energy variation over time and scale. In this work, we explore identifying and detecting reoccurring signal patterns during ventricular arrhythmias that may assist clinicians to associate pathologies with specific average pattern distributions. The objective of this paper is to identify reoccurring signal patterns in arrhythmia episodes and develop a methodology to automate the identification process. This work uses the wavelet analysis to detect the occurrence of signal patterns during an arrhythmia segment. Though pattern correlation has been used to identify intra-cardiac electrogram patterns during ventricular tachycardia (VT) [6], wavelet analysis is better suited for pattern detection because of the natural scaling and translation of the wavelet. Analysis on the surface ECG is also more practical as these are readily available for diagnosis by clinicians. The paper provides details of the database, pattern identification and methodology in Section II, the results and discussion on the contributions in Section III followed by conclusions in Section IV.

Thanks to NSERC for funding this work.

[1]K. Balasundaram and K. Umapathy is with Department of Electrical and Computer Engineering, Ryerson University, Toronto, Canada karthi@ee.ryerson.ca

[2]S. Masse and K. Nair is with Toronto General Hospital, Toronto, Canada

II. Method

A. Database

Fourteen ECG segments (with an average duration of 3.24 $\pm$ 3.15 minutes) during ventricular arrhythmia were extracted from the MIT-BIH database [7] for the purpose of pattern identification and detection. These signals were sampled at 250 Hz and belonged to patients with varying arrhythmia conditions. The filtering of the ECG segment (filtered between 0.5 Hz and 30 Hz) and the energy normalization were the only pre-processing techniques applied to the database prior to the pattern identification stage. The 14 ECG segments consists of 9 VF segments and 5 VT segments. VT and VF account for a majority of ventricular arrhythmias, and were only chosen to limit the pattern selection to the most common types of ventricular arrhythmias.

B. Pattern Identification

The 14 ECG segments from the MIT-BIH database were visually analyzed to detect reoccurring signal patterns. The signal patterns were searched over many ventricle depolarization complexes. The patterns were grouped into either local or global pattern. A local pattern is defined as a pattern that is a variation of a local depolarization. A global pattern is defined as a pattern that occurs over multiple depolarizations. If a signal pattern is observed to reoccur, it was first classified either as a local or global pattern. A pattern was said to reoccur if it had at least an average of 10 occurrences

978-1-4577-0216-7/13/$26.00 ©2013 IEEE

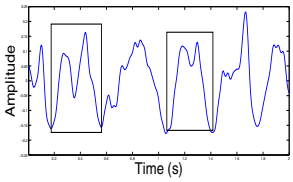

(a) Local Pattern 1

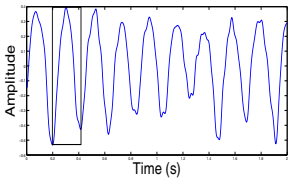

(b) Local Pattern 2

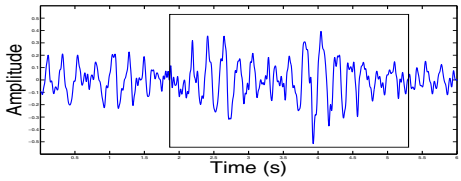

(c) Global Pattern

Fig. 1: Two local patterns and one global pattern

per minute over the entire database. Following the above procedure, we had identified 3 reoccurring patterns using the given database. Of the three patterns, two were identified as local patterns and one as a global pattern. The three identified patterns are presented in Figure 1.

The identified patterns given in Figure 1 may not be the only patterns, but these were found to be the most reoccurring patterns for the database analyzed. Patterns during normal sinus rhythm were not considered in this analysis. The identified patterns were found to have similarities to previously identified morphological patterns in intra-cardiac/implantable cardioverter defibrillator electrogram tracings in literature.

- **Local Pattern 1 (LP1) -** This pattern shown in Figure 1a has similarities to "double potential" that were observed in the intra-cardiac electrograms in the close vicinity of conduction blocks [8].
- **Local Pattern 2 (LP2) -** This pattern shown in Figure 1b has similarities to a single depolarization in a monomorphic VT signal.
- **Global Pattern (GP) -** This pattern resembles an amplitude modulated sinusoid (illustrated in Figure 1c). The GP can be seen as a transition from low signal amplitude to high signal amplitude and back to low signal amplitude. This morphology of changing amplitude during VF has also been previously reported in literature [9].

Following the manual identification of the patterns, our next step was to develop an accurate automated pattern detection technique such that these patterns can be detected at ease over larger databases or longer ECG records.

C. Pattern Detection

The wavelet transform was selected due to its ability to naturally scale and translate the mother wavelet to best match the ECG signal. In wavelet analysis, a signal $f(n)$ is modeled by varying the mother wavelet ψ. Due to the flexibility in generating many variations (scale and translation of the mother wavelet), wavelet decomposition is highly adaptive to

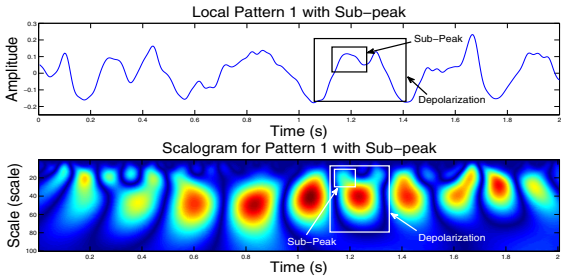

Fig. 2: Time-scale plane depiction of the LP1 (with the illustration of depolarization and sub-peak)

the signal structures. In addition, the flexibility in selecting the mother wavelet determines the characteristics of the decomposition and helps in performing signal adaptive and application specific analysis. The discrete implementation of continuous wavelet transform is given by Equation 1 [10],

$$Wf(s,m) = \frac{1}{\sqrt{s}} \sum_{n=1}^{N} f(n)\psi^*\left(\frac{n-m}{s}\right) \qquad (1)$$

where m and s represent the discretized translation and scale parameter and $Wf(s,m)$ represents the wavelet coefficients for the discrete time signal $f(n)$. The continuous wavelet transform was selected over the discrete wavelet transform because it is less affected by the translation of a pattern [11]. In order to capture the local and global patterns, the complex Gaussian wavelet was used because of its similarities to the depolarization found in ventricular arrhythmias. While the wavelet analysis was applied directly on the local pattern ECG, in order to detect the GP, the ECG was rectified to help identify the envelope.

Let the real, phase and normalized scalogram (squared magnitude) coefficients of the wavelet decomposition be represented as $Wf_r(s,m)$, $Wf_p(s,m)$ and $\tilde{Wf}(s,m)$. Detection of the individual depolarization was achieved by identifying maximas in the real coefficients ($Wf_r(s,m)$) using the eight-connected neighbourhood approach [12]. The phase coefficients ($Wf_p(s,m)$) was used to identify the peak and valley of a depolarization. Figures 2 and 3 depict the corresponding real valued coefficients ($Wf_r(s,m)$) for LP1 and the GP. In order to distinguish the local patterns, the characteristic identified was that the LP1 had sub-peaks within the depolarization, while LP2 did not have a sub-peak. The sample illustration depicting LP1 (Figure 2) highlights the depolarization with a sub-peak. The characteristic of the GP used for identification was the presence of its envelope, which is shown in Figure 3. Characteristics for each pattern were obtained based on analyzing the 14 ECG segments from the MIT database.

The scalogram ($\tilde{Wf}(s,m)$) along with the real and phase coefficients were used to detect the above discussed characteristics for each pattern. For the local patterns, the sub-peaks (or lack there of for LP2) were identified using the real and phase coefficients. Once the sub-peak and depolarizations were captured, a relative ratio between the sub-peaks and the depolarization was computed using the scalogram to identify its occurrence. These relative ratios were database specific as

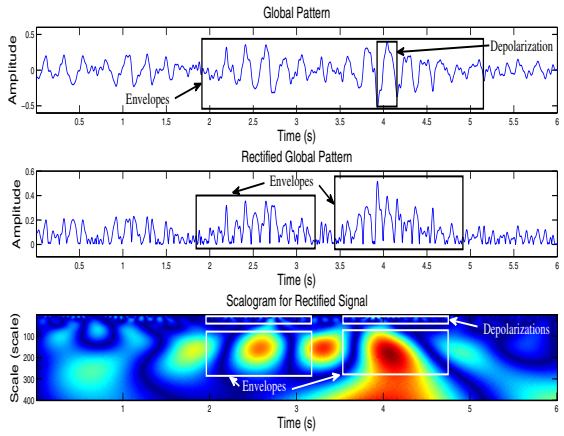

Fig. 3: Time-scale plane depiction of the GP (with the illustration of the envelope)

they were derived using a subset of the MIT database. Based on the sub-peak and depolarization analysis, a sub-peak was identified if it satisfied Equation 2.

$$\delta_1 \leq \frac{\tilde{Wf}_{sub-peak}}{\tilde{Wf}_{depol}} \times 100 \leq \delta_2 \tag{2}$$

The terms $\tilde{Wf}_{sub-peak}$ and $\tilde{Wf}_{depol}$ are the sub-peak and depolarization wavelet magnitudes respectively. The thresholds δ_1 and δ_2 were obtained experimentally by analyzing the 14 ECGs that had these patterns occurring. Once all the sub-peaks were identified for a particular depolarization, then a classification of the depolarization was made based on the presence (two sub-peaks for LP1) or absence (no sub-peaks for LP2) of the sub-peaks.

In the case of the GP, the envelope was first detected using the real and phase scalograms. Within the envelope, the depolarization to envelope ratio was obtained from the scalogram for each depolarization and then an average depolarization to envelope ratio was calculated. The GP was identified if the average ratio satisfied Equation 3.

$$\delta_3 \leq \frac{\sum_{n=1}^{N} \frac{\tilde{Wf}_{depol,n}}{\tilde{Wf}_{envelope}} \times 100}{N} \leq \delta_4 \tag{3}$$

From Equation 3, $\tilde{Wf}_{depol,n}$ is the n^{th} depolarization magnitude, $\tilde{Wf}_{envelope}$ is the envelope magnitude and N is the total number of depolarizations identified within the envelope. The thresholds δ_3 and δ_4 were also obtained experimentally by analyzing the 14 ECGs that had the GP occurring. Using this method, if the ratio for the local patterns or global pattern were within their respective thresholds, then the three identified patterns were automatically detected. This information could be used to represent the arrhythmia as a percentage of distribution for these patterns.

III. Results and Discussion

In order to validate the automated detection process, the 14 ECG segments were manually validated with the patterns that were detected automatically. The number of automatically detected patterns were verified against manually identified patterns to determine the detection accuracies of each pattern using the proposed method. The detected patterns were averaged for the 14 ECG segments as occurrence per minute. The detection accuracies for the patterns are given in Table I. A detection accuracy of 73.3%, 75.0% and 86.6% were achieved for LP1, LP2, and the GP respectively. This identification was also verified by two independent observers on a subset of the database and achieved an overall accuracy of 70.5% and 71.5% respectively.

The above validated automated detection process was applied to compute the distribution of these patterns for all the 14 ECG segments. To demonstrate that the distribution of these patterns are different for the two types of ventricular arrhythmias and also that they differ within VF, we performed two separate comparisons. The first comparison, we segregated the 14 ECG segments into the 9 VF and 5 VT segments and computed the percentage of energy captured by each pattern. Figure 4 shows the average energy captured by each pattern for VF and VT segments. Although VT and VF classification can be performed using many existing methods, the motivation here is to highlight the differences between the distribution in the occurrence of the proposed patterns between the ventricular arrhythmias. The mean and standard deviation for the patterns are highlighted in Table II.

Analyzing the differences in the pattern distribution among the ventricular arrhythmia group (VT and VF), it is evident that LP1 and GP can easily discriminate between VT and VF. Observing the occurrence of these pattern in VT and VF, LP1 seems to occur more during VF, as shown in Figure 4a, and LP2 seems to occur more in VT, as shown in Figure 4b. It should be noted that there are some similarities in the occurrence of the GP in both VT and VF (as observed in Figure 4c). This is likely the result of the difficulty in distinguishing the GP from torsade de pointes, which has been previously reported [13]. While monomophic VT may not have LP1 or GP occurring, it is possible for these patterns to occur in polymorphic VT, which explain the observations of these patterns in the VT samples analyzed.

TABLE I: Automated Pattern Detection Validation Accuracies Based on Average Occurrence per Minute

Pattern	Manual	Automated	% Accuracy
LP 1	16.09	11.79	73.3%
LP2	85.56	64.17	75.0%
GP	11.83	10.24	86.6%

TABLE II: Group Mean and Standard Deviation for Each Pattern

Group	VT	VF
LP1	3.0% (± 2.2%)	7.6% (± 4.2%)
LP2	39.0% (± 27.1%)	27.1% (± 11.5%)
GP	29.4% (± 22.6%)	42.3% (± 19.2%)

In the second comparison, our intention was to demon-

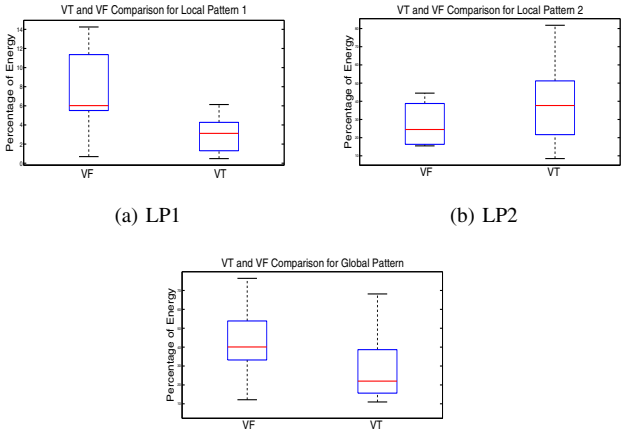

(a) LP1 (b) LP2

(c) GP

Fig. 4: Pattern comparison between VT and VF

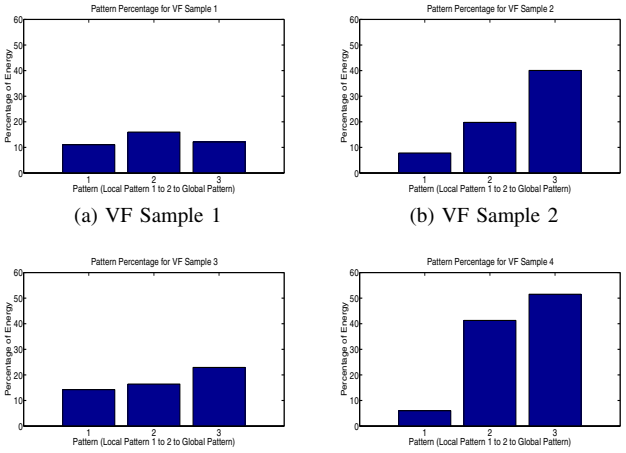

(a) VF Sample 1 (b) VF Sample 2

(c) VF Sample 3 (d) VF Sample 4

Fig. 5: Pattern Distribution Among Four VF Samples

strate that even within the same type of ventricular arrhythmia, there are variations in the distribution of these patterns. In order to demonstrate this, we have presented the histogram of the three patterns for four different VF segments.

Upon closely analyzing pattern distributions among the VF samples in Figure 5, we note that VF Sample 1 and VF Sample 3 (Figures 5a and 5c) have similarities in the distribution of the patterns and likewise VF Sample 2 and VF Sample 4 (Figures 5b and 5d) have similarities in the distribution of the patterns. VF sample 1 and VF sample 3 (Figure 5a and 5c) have a relatively low occurrence of LP2 and GP but a relatively higher occurrence of LP1 when compared with VF sample 2 and VF sample 4. Therefore, this information might be highly valuable if these patterns could be associated with underlying pathologies.

The demonstration that the proposed approach could highlight the differences between and within ventricular arrhythmias using single channel ECG signal patterns opens up the possibilities of characterizing ventricular arrhythmias in terms of signal morphologies. These patterns could provide an indication of the state of the heart or nature of pathologies that could assist clinicians to provide targeted diagnosis and treatment. If the link between such reoccurring signal patterns and the spatio-temporal organizational centers (which needs high resolution 2D mapping) during ventricular arrhythmias could be established this may motivate catheter ablation based therapies where usually the clinicians only has access to a few electrogram channels.

IV. Conclusions

We have presented three commonly reoccurring signal patterns in ECG during ventricular arrhythmias and a wavelet based technique for automatically identifying these patterns. Identifying and analyzing the distribution of these patterns could assist clinicians in associating pathologies and subclassifying the affected population which may lead to better targeted diagnosis and treatment. By creating a knowledge base of ventricular arrhythmia signal patterns, an expert system could be developed that could assist in characterizing ventricular arrhythmias. Future work involves testing the proposed patterns in a larger database and perform subgroup classifications in associating clinical information to the occurrence of signal patterns.

References

[1] Z. Zheng, J. Croft, W. Giles, and G. Mensah, "Sudden cardiac death in the united states, 1989 to 1998," *Circulation*, vol. 104, no. 18, pp. 2158–2163, 2001.

[2] G. Moe, "On the multiple wavelet hypothesis of atrial fibrillation." *Arch Int Pharmacodyn Ther*, vol. 140, p. 183, 1962.

[3] K. Ten Tusscher, A. Mourad, M. Nash, R. Clayton, C. Bradley, D. Paterson, R. Hren, M. Hayward, A. Panfilov, and P. Taggart, "Organization of ventricular fibrillation in the human heart: experiments and models," *Experimental physiology*, vol. 94, no. 5, p. 553, 2009.

[4] K. Balasundaram, S. Masse, K. Nair, T. Farid, K. Nanthakumar, and K. Umapathy, "Wavelet-based features for characterizing ventricular arrhythmias in optimizing treatment options," in *Engineering in Medicine and Biology Society, EMBC, 2011 Annual International Conference of the IEEE*. IEEE, 2011, pp. 969–972.

[5] K. Balasundaram, S. Masse, K. Nair, and K. Umapathy, "A classification scheme for ventricular arrhythmias using wavelets analysis," *Medical and Biological Engineering and Computing*, pp. 1–12, 2012, DOI 10.1007/s11517-012-0980-y.

[6] E. Treo, D. Cervantes, and E. Ciaccio, "Automated detection and mapping of electrical activation when electrogram morphology is complex," *Biomedical Signal Processing and Control*, 2012.

[7] A. L. Goldberger, L. A. N. Amaral, L. Glass, J. M. Hausdorff, P. C. Ivanov, R. G. Mark, J. E. Mietus, G. B. Moody, C.-K. Peng, and H. E. Stanley, "PhysioBank, PhysioToolkit, and PhysioNet: Components of a new research resource for complex physiologic signals," *Circulation*, vol. 101, no. 23, pp. e215–e220, 2000.

[8] F. Evans, J. Rogers, W. Smith, and R. Ideker, "Automatic detection of conduction block based on time-frequency analysis of unipolar electrograms," *Biomedical Engineering, IEEE Transactions on*, vol. 46, no. 9, pp. 1090–1097, 1999.

[9] W. Hsu, Y. Lin, J. Heil, J. Jones, and D. Lang, "Effect of shock timing on defibrillation success," *Pacing and clinical electrophysiology*, vol. 20, no. 1, pp. 153–157, 1997.

[10] L. Angrisani, P. Daponte, M. D'apuzzo, and A. Testa, "A measurement method based on the wavelet transform for power quality analysis," *Power Delivery, IEEE Transactions on*, vol. 13, no. 4, pp. 990–998, 1998.

[11] C. Burrus, R. Gopinath, and H. Guo, "Introduction to wavelets and wavelet transforms: A primer." *Recherche*, vol. 67, p. 02, 1998.

[12] D. Lowe, "Distinctive image features from scale-invariant keypoints," *International journal of computer vision*, vol. 60, no. 2, pp. 91–110, 2004.

[13] C. Opitz, G. Mitchell, M. Pfeffer, and J. Pfeffer, "Arrhythmias and death after coronary artery occlusion in the rat: continuous telemetric ecg monitoring in conscious, untethered rats," *Circulation*, vol. 92, no. 2, pp. 253–261, 1995.